MIMO Characterization of Indoor Wireless Optical Link Using a Diffuse-Transmission Configuration

Yazan A. Alqudah and Mohsen Kavehrad, *Fellow, IEEE*

***Abstract*—Performance of a diffuse optical link may potentially be degraded by temporal dispersions resulting from surface reflections. In order to devise techniques to alleviate the adverse effect of dispersion, an accurate channel model is needed. Obtaining the impulse response (IR) for a given receiver location requires not only consideration of direct path, but also reflections up to *n*th order. The IR is only valid for a specific location and specific receiver parameters. If a receiver moves, IR has to be recalculated. In this paper, we propose a new approach for characterizing diffuse links that both results in a tremendous saving in calculations and gives more insight on the channel characteristics. The new approach is based on consolidating the dependence of receiver parameters, transmitter parameters, and indoor environment into independent components. Thus, changing one of the parameters of the link requires recalculation of one of these components. The new model is utilized to obtain an accurate profile of delay spread and received power throughout a room.**

***Index Terms*—Channel modeling, diffuse configuration, indoor environment characteristics.**

I. Introduction

WIRELESS optical (infrared) link provides a secure and a promising alternative to radio for wireless indoor applications, be it for terminals or sensors [1]. The large spectrum of unregulated band enables a link to provide broadband access needed for multimedia and other bandwidth-demanding applications. The inability of the infrared light to pass through opaque obstacles provides interference-free bandwidth reuse in adjacent rooms. Susceptibility to shadowing, multipath dispersion, and limited range resulting from the noise generated by the ambient light are the main challenges in the design of an infrared link.

Several configurations are proposed for link design. These configurations are classified according to their directivity and line-of-sight (LOS). A link is referred to as directed if the receiver and the transmitter have a narrow radiation pattern and field-of-view (FOV), respectively. In a nondirected link, the transmitter has a broad radiation pattern and the receiver uses a large FOV. An LOS/non-LOS classification depends on whether or not an unobstructed path between a transmitter and a receiver exists.

Directed LOS link reduces path loss at the expense of disabling receiver mobility. The link can easily be lost if obstructed by an object. To solve this problem, nondirected non-LOS link (also known as diffuse) is used, where the optical power is projected onto a reflecting surface, chosen to be accessible to most receiver locations. The link does not require transmitter/receiver alignment, and thus provides robustness against link loss due to blockage. This configuration, however, suffers from a high path loss due to the absence of a direct path and data-rate limitation caused by reflections. This latter limitation results from multipath temporal dispersion caused by different paths (including reflections off of walls and ceiling) the signal takes to travel to a receiver.

To combat the adverse effects of temporal dispersion in high-speed applications, an accurate channel impulse response (IR) is needed. The impulse response is used to analyze and compensate for the effects of multipath dispersion. Researchers have proposed different approaches to obtain channel IR. Barry *et al.* [2] introduced a recursive method to compute the impulse response accounting for any number of reflections. A fast method to calculate multipath dispersion using Monte Carlo simulation that enables evaluation of Lambertian and other specular reflections is presented in [3]. In [4], a statistical approach to estimate channel IR of a diffuse source is studied to solve the computational complexity using an iterative approach. By slicing into time steps rather than into number of reflections, [5] proposed a fast algorithm for developing comparisons of pulse broadening for several sources and receivers, simultaneously.

Advancements in processing and storage of personal computers facilitate extending the method introduced in [2] to enable an efficient computation of impulse response between any number of transmitters and receivers. The method described here consolidates the parameters that determine the impulse response into four components: 1) source component contains dependence of impulse response on the source parameters; 2) environment component contains dependence on environment geometry, dimensions, and reflection coefficients; 3) receiver component contains dependence on receiver parameters; and finally, 4) direct component which accounts for direct response. Once calculated, these components are stored for future calculations. Changing parameters of one of the components (e.g., receiver/transmitter location) only affects the value of a single component. When the new value of the affected component is calculated, stored values of other components are used to evaluate a new impulse response. Impulse response dependence on transmitter and receiver components is linear; therefore, impulse response of a transmitter producing L diffusing elements can be calculated by evaluating a component equivalent to L elements. This is helpful when a link uses a large number of diffusing elements, as in diffuse configuration.

Paper approved by K. Kitayama, the Editor for Optical Communication of the IEEE Communications Society. Manuscript received October 8, 2002; revised April 5, 2003.

The authors are with the Center for Information and Communications Technology Research (CICTR), Department of Electrical Engineering, The Pennsylvania State University, University Park, PA 16802 USA (e-mail: mkavehrad@psu.edu).

Digital Object Identifier 10.1109/TCOMM.2003.816945

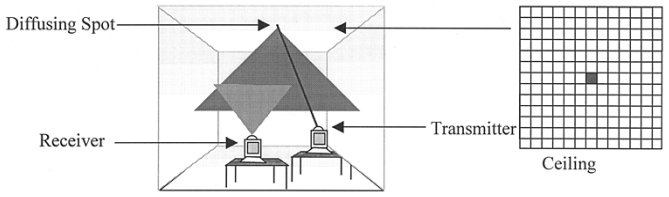

Fig. 1. Single-element diffusing configuration.

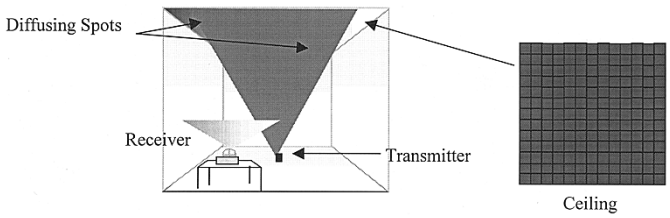

Fig. 2. Diffuse link. A transmitter placed at room center is used to illuminate the ceiling.

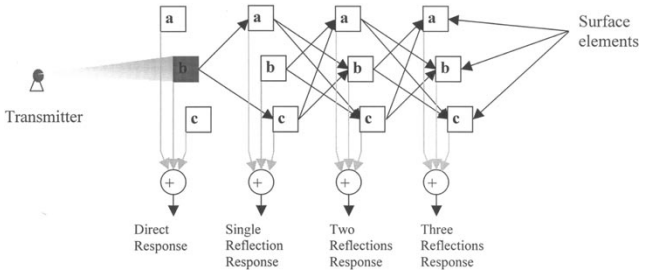

Fig. 3. Illustration of signal propagation. The room surface is composed of three elements: **a, b,** and **c**. A transmitter illuminates element **b**. The impulse response of any reflection is found by considering all the elements within the receiver FOV. In this example, all the elements are within the receiver FOV. Complexity in calculating impulse response is caused by reflections. Each reflection results in $N-1$ new reflections.

It is often the case, when designing a link, that only one of the components changes. For instance, the objective might be to calculate the impulse response for a given transmitter configuration at different locations within a room. In this case, an equivalent source-environment component is calculated and used, with the varying receiver component, to obtain an impulse response. This results in tremendous saving in computation time.

This paper is organized as follows. In Section II, we introduce two configurations that are considered in the study. Section III discusses the channel model, and the complexity involved in calculating impulse response. In Section IV, a new approach to channel modeling is presented. The results of simulation of the impulse response using the proposed approach are provided in Section V. Concluding remarks are presented in Section VI.

II. Link Configuration

The two link configurations considered in this study are single-element diffusing and nondirected non-LOS. Although, a single-element diffusing is a hypothetical configuration, its consideration serves as a benchmark in deriving the model of nondirected non-LOS. Therefore, we present it as a separate configuration.

A. Single-Element Diffusing

In a single-element diffusing configuration, a transmitter generates a diffusing spot on a reflecting surface, which acts as a Lambertian reflector. Thus, the diffusing spot behaves as a wide-beam transmitter. A receiver with large FOV is used to ensure an LOS component in the impulse response as illustrated in Fig. 1. The configuration differs in functionality from directed non-LOS in that a receiver is assumed to have a wide FOV. It also differs from nondirected LOS in not requiring a path between a transmitter and a receiver.

B. Nondirected Non-LOS (Diffuse)

The nondirected non-LOS is a generalization of single-element diffusing. The transmitter produces diffusing elements on the entire ceiling, as illustrated in Fig. 2. A large FOV receiver is used to reduce path loss. The diffuse link enables one-to-many communication without the need for receiver alignment.

III. Channel Model

The complexity in obtaining channel IR is brought about by the multiple paths signals take in traveling from a transmitter to a receiver. This multipath results from reflections off of walls, ceiling, furniture, etc. Room surfaces act as Lambertian reflectors that reflect an incident signal in all directions. Assuming room surface exposed to a transmitter is made of N surface elements, each reflection produces $N-1$ new reflections, as illustrated in Fig. 3. When determining channel IR, contribution of each element on a surface within receiver FOV should be considered. Since surfaces do not offer perfect reflection and signal strength is inversely proportional to the distance traveled, a finite number of reflections is considered in obtaining an impulse response.

Impulse responses are obtained by dividing the reflecting surface into a finite number of reflecting elements N [2]. If N is large, accurate samples of continuous impulse response are obtained. The number of elements N for a rectangular room, of dimensions equal to (W, L, H), is given by

$$N = 2 \times (n_x \times n_z + n_x \times n_y + n_y \times n_z) \tag{1}$$

where

$$\frac{W}{n_x} = \frac{L}{n_y} = \frac{H}{n_z} = d.$$

Constant d represents the distance between centers of neighboring elements, which is taken to be the same for all surfaces. Every surface element contributes directly to the received signal if that element is within receiver FOV, or indirectly through reflections off other surfaces, as illustrated in Fig. 3. The radiation pattern of diffuse elements, as well as surface elements, is assumed first-order Lambertian. The LOS response $\mathrm{h}^0(\mathrm{t})$, when the source T is within the FOV of the receiving element R can be expressed as [2]

$$h_{TR}^0(t) = \frac{\cos(\varphi_{TR}) \cdot \cos(\theta_{TR}) \cdot A_R}{\pi \cdot {R_{TR}}^2} \delta\left(t - \frac{R_{TR}}{c}\right) \tag{2}$$

where $\cos(\varphi_{TR})$ is equal to dot product of two unit vectors. The first is perpendicular to T, and the second originates from R and

extends toward T. The angle θ_{TR} is the angle between a vector perpendicular to R and a vector that lays on the straight line that connects T and R. A_R is the receiving element area, R_{TR} is the distance between T and R, and c is the speed of light. The response after a single reflection off an element i is obtained by treating i as a receiver, and then as a source. The impulse response is given by

$$h^1_{TR}(t) = \frac{\cos(\varphi_{Ti})\cos(\theta_{Ti})A_i}{\pi {R^2}_{Ti}} \frac{\rho_i \cos(\varphi_{iR})\cos(\theta_{iR})A_R}{\pi {R_{iR}}^2} \times \delta\left(t - \frac{R_{Ti} + R_{iR}}{c}\right) \quad (3)$$

where A_i is the area of the reflecting element i, and ρ_i is its reflectivity. The response resulting from two reflections off element i first and then off element j is found by extending (3) to include impulse response between j and the receiver, and is expressed as

$$h^2_{i,j,R}(t) = \frac{\cos(\varphi_{Ti})\cos(\theta_{Ti})A_i}{\pi {R^2}_{Ti}} \times \frac{\rho_i \cos(\varphi_{ij})\cos(\theta_{ij})A_j}{\pi {R_{ij}}^2} \times \frac{\rho_j \cos(\varphi_{jR})\cos(\theta_{jR})A_R}{\pi {R^2}_{jR}} \delta\left(t - \frac{R_{Ti} + R_{ij} + R_{jR}}{c}\right). \quad (4)$$

Higher reflections impulse response is obtained by adding impulse response of new reflections similar to (4). It is apparent, however, that as more reflections are considered, received power becomes smaller. This is the case since nth order impulse response is equal to $n-1$th order multiplied by a quantity that is much smaller than one.

Total impulse response is obtained by summing direct and reflection responses. In doing so, all surface elements must be considered. In calculating the second reflection response, for instance, N values are used for both i and j in (4) and the resultant second reflection response is the sum of $N \times N$ responses. Therefore, calculation complexity is directly proportional to the number of surface elements raised to the number of reflections considered. The impulse response obtained is only valid for a specific transmitter/receiver configuration. Changing any of the transmitter/receiver parameters requires the calculations to be performed again. When studying a communication link, we are interested in obtaining impulse responses for a large set of receiver/transmitter parameters. Obtaining the delay spread profile, for instance, requires the calculation of impulse response for hundreds of receiver locations. Performing the above calculations can become prohibitively intensive. It can easily be recognized that many calculations involved in obtaining the impulse response do not change. In the next section, we propose a new representation of transmitter-channel-receiver that makes efficient use of calculations performed. The new representation also provides more insight into the channel characteristics.

IV. Multi-Input Multi-Output (MIMO) System

In the new model, the transfer function between a transmitter and a receiver is divided into four components. The first represents the transfer function between a source and surface elements. The second block contains the transfer function between surface elements. The third has the transfer function from surface elements to a receiver. The last component accounts for direct response between a source and a receiver. A similar approach of dividing signal path is presented in [5].

In our discussion, we assume geometry as well as reflection coefficients are fixed, and the room internal surface is made up of N neighboring elements of equal area. Elements are numbered sequentially, and each element is identified by an index. We refer to diffusing spots as sources and the device generating them as transmitter. The number of reflections is counted from a source to a receiver.

A. Source Profile (F)

The first component in the new model represents transfer function between source (diffusing spot) and surface elements. It is referred to as source profile and is modeled by a single-input multiple-output system with N outputs. The transfer function between a source and each of the surface elements is expressed by an entry in a vector F_s. Since surface elements 1 through N receive the signal directly, the transfer function f_{sk} between a source s and element k, is obtained using (2), and is given by

$$f_{sk} = \rho_k \delta\left(t - \frac{R_{Ts}}{c}\right) \frac{\cos(\theta_{sk})\cos(\varphi_{sk})A_R}{\pi \cdot {R_{sk}}^2} \times \delta\left(t - \frac{R_{sk}}{c}\right) u\left(\frac{\pi}{2} - \theta_{sk}\right) \quad (5)$$

where the first two terms are added to account for the transfer function between a transmitter and a source. For a single source s, the vector F_s is expressed as

$$F_s = [f_{s1} \cdots f_{sN}]. \quad (6)$$

The expression can be extended to include more than a single source. In the case of a diffuse link, where transmitter illuminates ceiling, the equivalent vector F_{eq} is defined as the equivalent of $n_x \times n_y$ sources and is given by

$$F_{\text{eq}} = \sum_{i=1}^{n_x \times n_y} F_i = [f_{\text{eq}1} \cdots f_{\text{eq}N}] \quad (7)$$

where $f_{\text{eq}} = \sum_{i=1}^{n_x \times n_y} f_{ij}$. The source vector is shown as block F_s in Fig. 4(a).

B. Environment Matrix (Φ)

The second component consolidates dependence on indoor geometry, dimensions, and reflection coefficients. This component contains the transfer functions between any two reflecting elements. In matrix format, and considering up to n reflections, it is expressed as

$$\Phi_n = \begin{cases} I_{N\times N} + \phi + \phi^2 + \phi^3 + \cdots \phi^{n-1}, & n \geq 2 \\ I_{N\times N}, & n = 1 \end{cases} \quad (8)$$

where $I_{N\times N}$ is the $N \times N$ identity matrix, and ϕ is given by

$$\phi = \begin{bmatrix} \phi_{11} & \cdots & \phi_{1N} \\ \vdots & \ddots & \vdots \\ \phi_{N1} & \cdots & \phi_{NN} \end{bmatrix}. \quad (9)$$

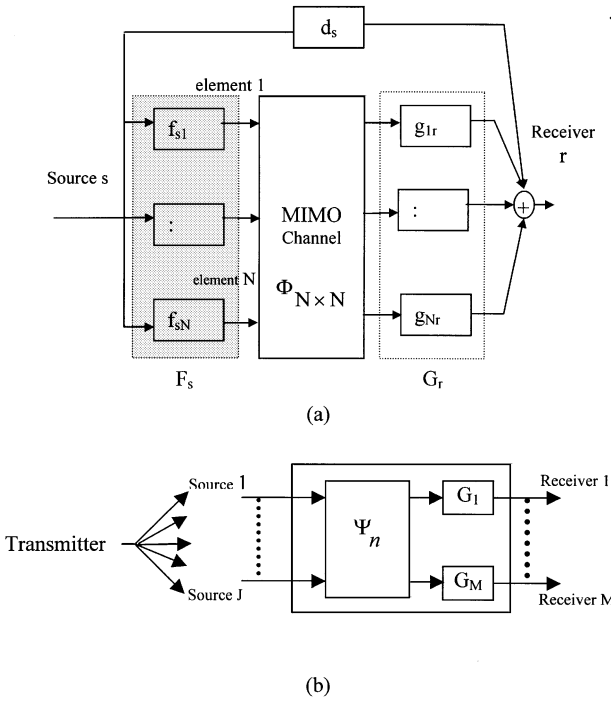

Fig. 4. (a) New representation of impulse response for a single source and a single receiver. (b) Representation of J sources and M receivers.

The entry ϕ_{ik} represents transfer function between two elements i and k, and is given by

$$\phi_{ik}=\begin{cases} 0, & i=k \\ \dfrac{\rho_i \cos\theta_{ik}\cos\varphi_{ik}A_k}{\pi R_{ik}^2}\delta\left(t-\frac{R_{ik}}{c}\right)u\left(\frac{\pi}{2}-\theta_{ik}\right), & i\neq k. \end{cases} \tag{10}$$

The environment matrix is independent of transmitter and receiver, once calculated; it can be used with any transmitter/receiver configuration.

C. Receiver Profile (G)

This component contains impulse response dependence on receiver parameters such as location and FOV. It is represented by block G_r in Fig. 4. The block contains transfer functions between a receiver and N surface elements. In vector form, it is expressed as

$$G_r = \begin{bmatrix} g_{1r} \\ \vdots \\ g_{Nr} \end{bmatrix} \tag{11}$$

where the entry g_{ir} is given by

$$g_{ir} = \frac{\rho_i \cos\theta_{ir}\cos\varphi_{ir}A_r}{\pi R_{ir}^2}\delta\left(t-\frac{R_{ir}}{c}\right)u(\mathrm{FOV}_r-\theta_{ir}). \tag{12}$$

The number of nonzero elements in G_r is directly proportional to the receiver FOV. The symmetry of the G vector is lost when the receiver is located close to more than one surface, each in a different plane.

D. Direct Response Vector (D)

When a source is within a receiver FOV, a direct response results. This response is expressed as

$$H^{(0)} = D \cdot G_r \tag{13}$$

where D is a $1 \times N$ vector given by

$$D = [d_1 \cdots d_N]. \tag{14}$$

The entry d_i is equal to $\delta(t-(R_{Ti}/c))$ if an element i corresponds to a diffusing spot, and 0, otherwise. R_{Ti} accounts for the delay between transmitter and source i. In diffuse configuration, there are $n_x \times n_y$ nonzero elements in D. The direct response is represented by block d_s in Fig. 4(a).

E. Total Response (H)

The total impulse response H between a source s and a receiver when n reflections are considered can be expressed as

$$\begin{aligned} H &= \sum_{i=0}^{n} H^{(i)} \\ &= D \cdot G_r + F_s \cdot \Phi_n \cdot G_r \end{aligned} \tag{15}$$

If a vector Ψ_n that contains N entries is defined as

$$\Psi_n = D + F_s \cdot \Phi_n \tag{16}$$

H can be written as

$$H = \Psi_n G_r. \tag{17}$$

The matrix Ψ_n contains the signals seen by each element of room surface. By multiplying by G_r, the signal is shifted to account for the delay between elements and receiver and multiplied by a factor that depends on the path between each element and receiver. The expression for H in (17) readily applies to a diffuse link by substituting for F the F_{eq}.

One of the advantages attained by the new model is highlighted in (17). In analyzing an impulse response link, we are often interested in the impulse response for many receiver locations within a room. Room parameters do not change, nor do parameters of the transmitter, only parameters of the receiver change. Using (17) to calculate a new impulse response requires calculating the new value of G_r and multiplying by Ψ_n, which is already calculated. This is illustrated for M receiver locations in Fig. 4(b). The time required for calculating Ψ_n is comparable to that required to calculate a single impulse response. Once Ψ_n is calculated and stored, however, the time required to calculate a new impulse response is reduced to calculating the multiplication of two matrices, which takes a very short time.

The new model can result in time saving even when a single impulse response is calculated. By calculating receiver vector G_r first, the elimination of any unnecessary calculation is possible. This is especially true when the receiver FOV is small, since the nonzero entries in G_r are a small fraction of total entries. When the kth entry in G_r is zero, the corresponding kth column in Ψ_n does not affect the calculation since it is multiplied by zero. Therefore, for n nonzero entries in G_r, only corresponding n columns in Ψ_n have to be calculated.

TABLE I
LINK PARAMETERS USED IN COMPUTER SIMULATIONS

Room Parameters	Diffuse
Width(W)	6 m
Length(L)	6 m
Height(H)	3 m
$\rho_{wall1}=\rho_{wall2}=\rho_{wall3}=\rho_{ceiling}$	0.7
$\rho_{wall4\ (Window)}$[6]	0.04
ρ_{floor}	0.2
Source Parameters	
Location (x,y,z)	Covering the ceiling
Number of spots	3600
Transmitter	
Location	(3.0,3.0,0.9)
Receiver Parameters	
FOV	90^o
Other Parameters	
d	0.2
N	3600

V. COMPUTER SIMULATION

In carrying out simulation on a personal computer, entries in the F, Φ, and G are represented as complex numbers with phase equal to time delay. Since delay takes on a very small value, it is expressed as an integer multiple of sampling time T_s. The value of T_s is chosen to be equal to the time it takes light to travel between two neighboring elements [2], i.e.,

$$T_s = \frac{d}{c}. \tag{18}$$

When performing addition, only terms that have equal delay are added together. Thus

$$ax^{-n_i} + bx^{-n_j} = \begin{cases} (a+b)x^{-n_i}, & i = j \\ ax^{-n_i} + bx^{-n_j}, & i \neq j. \end{cases} \tag{19}$$

The impulse response H_c is defined as received optical power when transmitted optical power is equal to a delta function with a unit area, i.e., $1W$ [1]. In order for area under the impulse response to be equal to received power, (15) is divided by T_s. The impulse response H_c resulting from matrix multiplication and simplification is in the form

$$\begin{aligned} H_c &= \left(\frac{1}{T_s}\right) \times [D \cdot G_r + F_s \cdot \Phi_n \cdot G_r] \\ &= h_0 x^{-n_0} + \cdots + h_{K-1} x^{-n_{K-1}} \end{aligned} \tag{20}$$

where h_i is the amplitude of the impulse response at time equal to $n_i \times T_s$. Environmental parameters used in computer simulation are summarized in Table I.

A. Received Power Per Reflection

The new model makes it possible to obtain received power for any order of reflection. Received power for a reflection order is defined as the area under impulse response of that reflection when $1W$ power is transmitted. In terms of the new model, this can be expressed as

$$P_i = \begin{cases} |F| \cdot |\Phi_i| \cdot |G|, & i \geq 1 \\ |D| \cdot |G|, & i = 0 \end{cases} \tag{21}$$

where $|x|$ denotes amplitude of x, and i is the reflection order. For the same receiver parameters, the amount of received power in each reflection depends on receiver location. When the receiver is close to a reflecting surface, the reflected power contributes more to the total receiver power. The average percentage of total power as more reflections are added for the environment considered in the simulation is shown in Fig. 5. The figure shows that on the average, more than 95% of total power is contained in the direct, first, second, and third reflections. In addition, the contribution of a reflection decreases as reflection order increases. As the complexity in calculating (8) grows as more reflections are considered. A tradeoff that guarantees 95% of total power is achieved by considering three reflections. Therefore, all the results below are calculated by considering direct response along with three reflections in the impulse response.

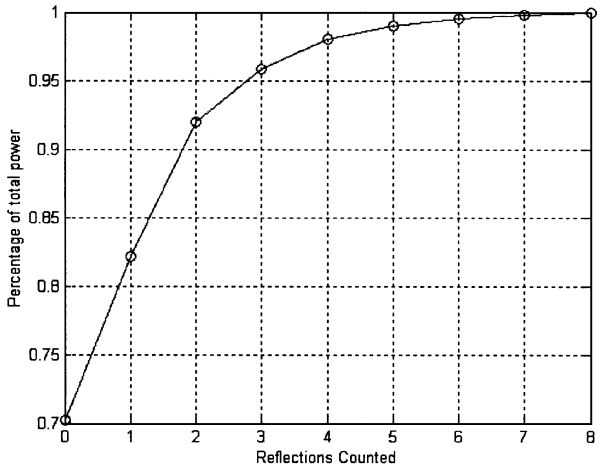

Fig. 5. Average percentage of total received power versus number of reflections. The average is calculated for 100 receiver locations. The link uses diffuse configuration.

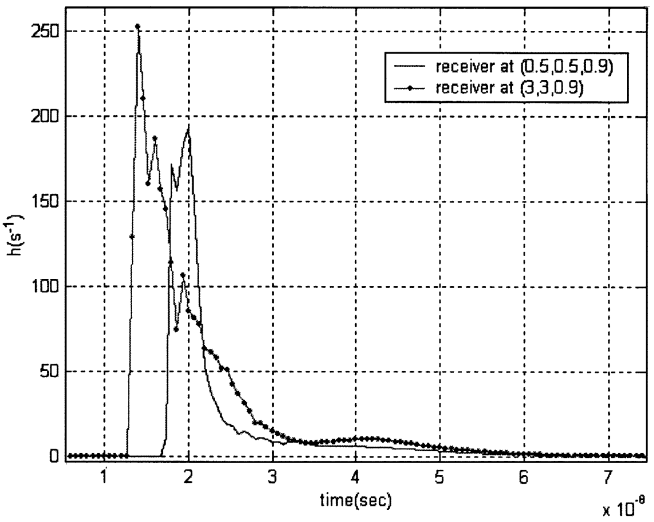

Fig. 6. Impulse responses of a diffuse link for receivers located at (0.5,0.5,0.9) and (3,3,0.9).

B. Impulse Response

The impulse responses of receivers, located at the room center and close to room corner, are shown in Fig. 6. The figure illustrates temporal dispersion, when a diffuse configuration is used.

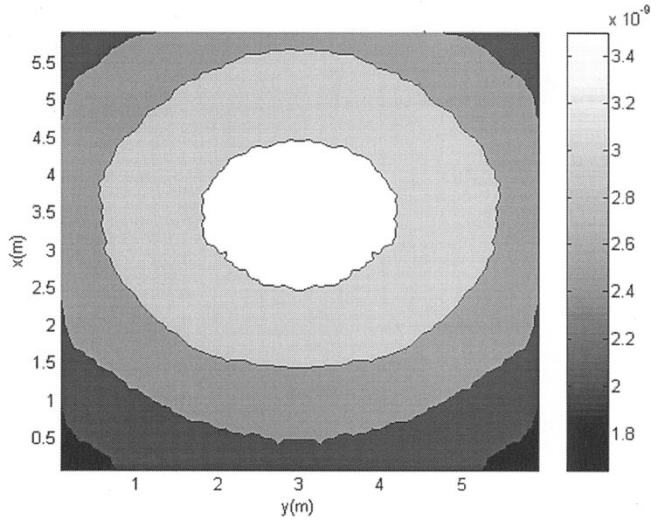

Fig. 7. Delay spread contour plot. The window wall is located at $x = 0$.

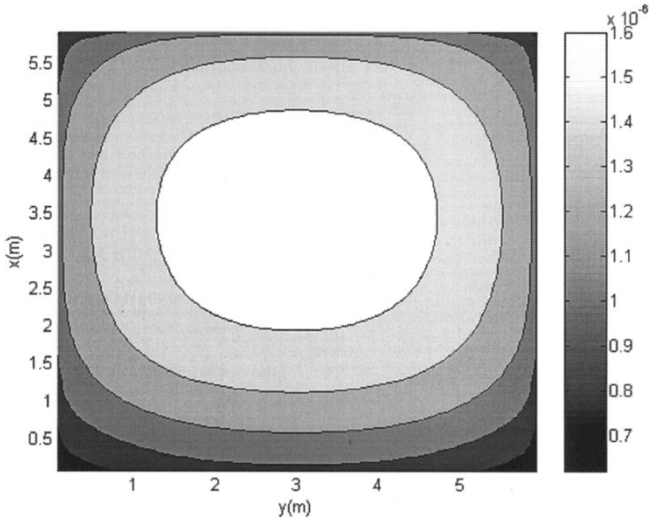

Fig. 8. Received power contour plot. The window wall is located at $x = 0$.

C. Delay Spread

Intersymbol interference resulting from propagation in a dispersive channel is a major problem in the design of a broadband wireless link. The dispersion in the channel sets the limit on the symbol length that can be used. As dispersion increases, symbols have to be placed at farther time intervals in order to reduce the adverse effect of dispersion [7]. This in turns reduces achievable bit rate. A measure of dispersion is provided by root mean square delay spread $T_{\text{delayspread}}$ defined as the second moment of the impulse response, and is given by [8]

$$T_{\text{delayspread}} = \sqrt{E(\tau^2) - (E(\tau))^2}. \tag{22}$$

In terms of H

$$E(\tau^n) = \frac{\sum_i \tau_i^n h_i^2}{\sum_i h_i^2} = \frac{\sum_{i=0}^{K-1} (i \times T_s)^n \times h_i^2}{\sum_{i=0}^{K-1} h_i^2}. \tag{23}$$

The profile of delay spread is shown in Fig. 7. The highest delay spread is shifted from the room center away from the wall covered by window; the spread decreases as receiver locations move away from the room center. Equal delay-spread locations belong to rings surrounding the maximum spread location. A total of 5776 receiver locations are considered in the computer simulations.

D. Received Power

Another measure of an optical link quality is provided by the total received power defined as the area underneath the impulse response curve

$$P_{\text{received}} = T_s \times \sum_{i=0}^{K-1} h_i \tag{24}$$

Received power provides a measure of attenuation for a transmitted signal due to propagation and reflections. The received power is related to path loss (PL) by [9]

$$\text{PL} = -10 \log_{10}[P_{\text{received}}]. \tag{25}$$

Fig. 8 shows the received power profile. Received power takes the highest value at a receiver location shifted from the room center away from the window. The power level falls as the receiver moves away from the maximum power location. The figure shows a small received power in the regions close to room corners. The regions of constant power are defined by rings surrounding the maximum power location.

VI. Conclusions

In this paper, a new representation of indoor optical link is introduced. The representation divides the physical path between a transmitter and a receiver into stages. Each stage consolidates a set of parameters upon which an impulse response depends. This results in a tremendous saving in calculation, especially when only one of the parameters is changed, such as location of a transmitter or a receiver.

The new representation enables us to calculate received power per reflection for a very high order of reflections. It is shown that the received power falls sharply with every new reflection. This justifies the consideration of the first few reflections when calculating an impulse response.

Temporal dispersion caused by multipath is one of the factors that limits achievable bit rate over a diffuse link. Through efficient calculation of impulse response, delay spread and received power profiles were generated. Both are obtained from channel IR. The matrix Ψ is calculated and stored in a file and is used to calculate impulse response at each new location. The time required to calculate Ψ is comparable to that required to calculate a single impulse response. Once Ψ is obtained, the calculation of a new impulse response requires less than 30 seconds.

References

[1] J. R. Barry, *Wireless Infrared Communications*. Norwell, MA: Kluwer, 1994.

[2] J. R. Barry, J. M. Kahn, W. J. Krause, E. A. Lee, and D. G. Messerschmitt, "Simulation of multipath impulse response for indoor wireless optical channels," *IEEE J. Select. Areas Commun.*, vol. 11, pp. 367–379, Apr. 1993.

[3] F. J. Lòpez-Hernàndez, R. Pèrez-Jimènez, and A. Santamaria, "Modified Monte Carlo scheme for high-efficiency simulation of the impulse response on diffuse impulse response wireless indoor channels," *Electron. Lett.*, vol. 34, no. 19, pp. 1819–1820, Sept. 1998.

[4] R. Pérez Jiménez, J. Berges, and M. J. Betancor, "Statistical model for the impulse response on infrared indoor diffuse channels," *Electron. Lett.*, vol. 33, no. 15, pp. 1298–1301, 1997.
[5] F. J. Lòpez-Hernàndez and M. J. Betancor, "DUSTIN: algorithm for calculation of impulse response on impulse response wireless indoor channels," *Electron. Lett.*, vol. 33, no. 21, pp. 1804–1806, Oct. 1997.
[6] J. B. Carruthers and J. M. Kahn, "Angle diversity for nondirected wireless infrared communication," *IEEE Trans. Commun.*, vol. 48, pp. 960–969, June 2000.
[7] M. R. Pakravan, M. Kavehrad, and H. Hashemi, "Indoor wireless infrared channel characterization by measurements," *IEEE Trans. Veh. Technol.*, vol. 50, July 2001.
[8] J. M. Kahn, W. J. Krause, and J. B. Carruthers, "Experimental characterization of nondirected indoor infrared channels," *IEEE Trans. Commun.*, vol. 43, pp. 1613–1623, Feb.-Apr. 1995.
[9] S. Jivkova and M. Kavehrad, "Multi-spot diffusing configuration for wireless infrared access," *IEEE Trans. Commun.*, vol. 48, pp. 970–978, June 2000.

Yazan A. Alqudah was born on August 3, 1971 in Ajloun, Jordan. He received the B.S degree from the University of Jordan, Amman, Jordan, in 1993 and the M.S. degree from Pennsylvania State University, University Park, in 1997, both in electrical engineering. He is currently working toward the Ph.D. degree at Pennsylvania State University.

From 1993 to 1994, he worked as a Lab Instructor at the Yarmouk University, Irbid, Jordan. From 1994 to 1997, he worked as a Teaching Assistant where he assisted with the design and building of experiments for the digital control laboratory. In 1997, he joined Schlumberger as an applications and software engineer. During his assignments, he was responsible for the personalization of subscriber identity modules (SIM) and over-the-air customization services for GSM carriers in North America. His current research interests include communication systems, channel modeling, and broadband optical wireless communication.

Mohsen Kavehrad (S'75–M'78–SM'86–F'92) received the Ph.D. degree from Polytechnic University (Brooklyn Polytechnic), Brooklyn, NY, in 1977 in electrical engineering.

Between 1978 and 1989, he worked on telecommunications problems for Fairchild Industries, GTE (Satellite and Laboratories), and AT&T Bell Laboratories. In 1989, he joined the University of Ottawa EE Department, as a full Professor. Since January 1997, he has been with the Pennsylvania State University EE Department as W.L. Weiss Chair Professor and founding Director of Center for Information and Communications Technology Research. He has over 250 published papers, several book chapters, books, and patents in wireless systems and optical networks. His current research interests are in wireless communications and optical networks.

Dr. Kavehrad received three Bell Labs awards for his contributions to wireless communications, the 1991 TRIO feedback award for a patent on an optical interconnect, the 2001 IEEE VTS Neal Shepherd Best Paper Award, three IEEE Lasers and Electro-Optics Society Best Paper Awards between 1991 and 1995, and a Canada NSERC Ph.D. dissertation award in 1995, with his graduate students. He is a former Technical Editor for the IEEE TRANSACTIONS ON COMMUNICATIONS, *IEEE Communications Magazine*, and the *IEEE Magazine of Lightwave Telecommunications Systems*. Presently, he is on the Editorial Board of the *International Journal of Wireless Information Networks*. He served as the General Chair of leading IEEE conferences and workshops. He has chaired, organized, and been on the advisory committee for several international conferences and workshops.